Metal–Semiconductor–Metal Traveling-Wave Photodetectors

Jin-Wei Shi, Kian-Giap Gan, Yi-Jen Chiu, Yen-Hung Chen, Chi-Kuang Sun, *Member, IEEE*, Ying-Jay Yang, and John E. Bowers, *Fellow, IEEE*

***Abstract*—We demonstrate a novel type of traveling wave photodetector: "metal–semiconductor–metal traveling-wave photodetecor" (MSM-TWPD). Demonstrated devices were fabricated using low-temperature grown GaAs (LTG-GaAs). In order to achieve high internal quantum efficiency, the narrow spacing between electrodes was fabricated by the self-aligned process without e-beam lithography. Electrooptical sampling measurement results at different optical pumping level are reported. Ultrahigh bandwidth (0.8-ps, 570-GHz transform bandwidth) performance was observed even under high optical power illumination (∼1.8 mW) with 8.1% net quantum efficiency. Compared with LTG-GaAs-based p-i-n TWPD and vertically illuminated MSM photodetector (PD), this novel TWPD has higher output saturation current with near terahertz electrical bandwidth, better quantum efficiency, and can be easily fabricated and integrated with other microwave devices. It thus promises the application in high-power distributed PD array or terahertz signal generation.**

***Index Terms*—Low-temperature-grown GaAs, metal–semiconductor–metal photodetectors, self-alignment, traveling-wave photodetectors, ultrahigh-speed photodetectors.**

HIGH-SPEED and high-sensitivity photodetectors have been studied extensively in the past ten years [1], owing to their application in broad-band optical communication network and optical generation of high-power microwave/millimeter waves [2]. Metal–semiconductor–metal (MSM) photodetectors [3], [4] and photoconductive switches deserve special attentions due to their high electrical bandwidth and ability of generating ultrashort electrical pulses [5], [6]. The bandwidth/efficiency product of traditional vertically illuminated MSM photodetectors is limited by the RC time constant, carrier drift time, and carrier recombination time. In order to shorten the carrier drift/recombination time, 25-nm finger spacing has been fabricated by using high-resolution e-beam lithography on low-temperature grown GaAs (LTG-GaAs) [3]. Although this device has a high bandwidth, it suffers relatively low quantum efficiency due to high metal–reflection loss. Besides, the fabrication process is expensive and complex. Another major problem for most vertically illuminated MSM photodetectors is RC bandwidth limitation. An alternative approach to overcome RC bandwidth limitation is traveling-wave photodetector (TWPD) [7]. In TWPD, the RC bandwidth limitation is replaced by velocity mismatch between the optical wave velocity V_o and the electrical wave velocity V_e [8]. A bandwidth of 560 GHz and a quantum efficiency of 8% have been reported using LT-GaAs on p-i-n structured TWPDs [9]. However, when the length of p-i-n-based TWPD is increased to get higher output saturation current (by reducing optical modal absorption constant), the bandwidth degrades seriously [10] due to large microwave loss and boundary reflection effect and the p-i-n TWPD will behave like an all-lumped type waveguide photodetector (WGPD) [11].

In this letter, we demonstrate a novel device: MSM traveling wave photodetector (MSM-TWPD). By utilizing LTG-GaAs and undoped-AlGaAs as photoabsorption and waveguiding layers, respectively, the dominant propagation microwave mode will be "quasi-TEM mode" instead of "slow wave mode" as in p-i-n-based TWPD structure [12]. The characteristics of low losses and high velocity in quasi-TEM microwave mode reduce the bandwidth degradation, comparing with p-i-n-based TWPD especially for long absorption length devices [11]. The fabricated devices exhibit high-speed performance, which have a 0.8-ps impulse response full-width at half-maximum (FWHM) and a 570-GHz transformed electrical bandwidth. By carefully designing the edge couple structure and utilizing self-aligned process to shorten the spacing between electrodes to hundreds of nanometers, 8.1% net quantum efficiency (including coupling loss) is achieved, which is higher than most LTG-GaAs-based photoconductive switch [5] or vertically illuminated MSM PDs [3] and is similar to the reported value of LTG-GaAs-based p-i-n TWPD [9].

The cross-sectional scheme of an MSM-TWPD is shown in Fig. 1(a). The structures of epilayers are composed by a thin LTG-GaAs layer (500 nm) for photoabsorption and two AlGaAs layers of 1 and 3 μm thickness, respectively. 1-μm-thick AlGaAs layer is the cladding layer for optical waveguiding and the 3-μm-thick AlGaAs layer is for optical isolation between the GaAs substrate and the LTG-GaAs active layer. The thin (100 Å) AlAs layer is to avoid As out-diffusion during annealing. The optical waveguiding in the x-direction is achieved by the etched-mesa ridge structure. Three metal stripes are electrodes to collect the photogenerated carriers in LTG-GaAs layer. The structure of three metal stripes acts as a co-planar waveguide (CPW), which supports a photoexcited

Manuscript received December 28, 2000; revised February 21, 2001. This work was supported by National Science Council of Taiwan, R.O.C., under Grant NSC 89-2215-E-002-064 and by the National Science Foundation under Award INT-9813411.

J.-W. Shi and Y.-H. Chen are with the Graduate Institute of Electro-Optical Engineering, National Taiwan University, Taipei 10617, Taiwan, R.O.C.

K.-G. Gan, Y.-J. Chiu and J. E. Bowers are with the Department of Electrical and Computer Engineering, University of California, Santa Barbara, CA 93106 USA.

C.-K. Sun is with the Department of Electrical Engineering and the Graduate Institute of Electro-Optical Engineering, National Taiwan University, Taipei 10617, Taiwan, R.O.C. (e-mail: sun@cc.ee.ntu.edu.tw).

Y.-J. Yang is with the Department of Electrical Engineering, National Taiwan University, Taipei 10617, Taiwan, R.O.C.

Publisher Item Identifier S 1041-1135(01)04557-8.

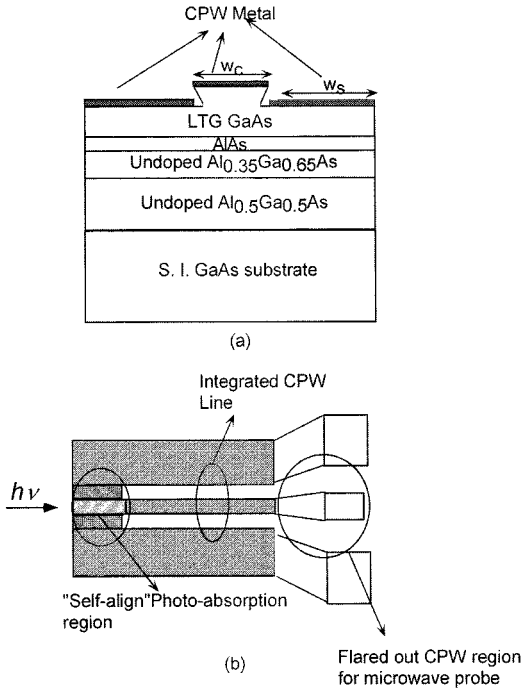

Fig. 1. (a) Cross-sectional diagram and (b) top view of MSM-TWPD. This structure can be easily fabricated by wet etching and self-aligned process. The integrated CPW line is for EO sampling measurement purpose.

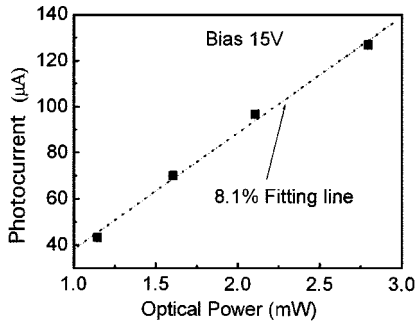

Fig. 2. Measured average photocurrent (solid squares) versus average optical input power. The bias voltage was 15 V. Dotted line is a linear fitting with 8.1% net quantum efficiency.

microwave guiding mode. The ground plane (with width w_s) is naturally separated from the center stripe (with width w_c) with the undercut profile of etched mesa (so-called self-aligned process). By utilizing the self-aligned process, the gap between metal stripes can be shortened to 200 $\sim$ 300 nm without e-beam lithography. There are some advantages for the narrow gapwidth of CPW line. Because of the narrow spacing between metal stripes, the carrier drift-time is shortened and the electric field strength is increased with enhanced internal quantum efficiency. Narrow gapwidth can also reduce the dominant microwave radiation loss, when operating in the ultrahigh frequency regime (several hundreds of gigahertz) [13]. Fig. 1(b) shows top view of the device. The length of device active region (self-aligned photoabsorption region) is 10 μm, and it is integrated with a CPW line in its output for electrooptical (EO) sampling measurement and dc biasing purposes.

The device fabrication process is discussed as follows. At first, the sample was annealing at 600 °C for 30 s for short carrier-trapping time and low dark current. By dipping in the mixture of NH_4OH, H_2O_2,H_2O (1 : 1 : 50) to remove the surface AlAs layer, the center stripe of CPW line was then fabricated on LTG-GaAs surface with standard photolithography, e-beam evaporation (Ti–Au, 10 nm/500 nm), and liftoff processes. The width of the center stripe was 2 μm. The metal stripe also served as the etch mask to form the optical ridge waveguide structure. The wet etchant for ridge structure was mixture of NH_4OH, H_2O_2,H_2O (3 : 1 : 100), which had an etching rate about 200 nm/min (with stirring) and could maintain good surface morphology after etching 300-nm-thick LTG-GaAs layer. After etching mesa, the ground planes of CPW line were directly evaporated by e-beam evaporation (Ti–Au, 5 nm/100 nm), which were naturally separated with the center metal stripe due to the 300-nm depth of the ridge waveguide structure. By utilizing self-aligned process, narrow spacing (hundreds of nanometers) between metal stripes could be easily achieved without e-beam lithography process. When the self-aligned photoabsorption region was finished, the LTG-GaAs layer was removed in other area of the device to avoid undesired absorption in measurement. Finally, the device was integrated with a CPW line on undoped AlGaAs layer for EO sampling measurement purpose. The widths of the center stripe and air gap of the integrated CPW line were 4 and 5 μm, respectively, which had a characteristic impedance of 60 Ω. The characteristic impedance in the self-aligned photoabsorption region was around 30 Ω. Although there was an impedance mismatch between detector and integrated CPW line in our fabricated device, the round-trip frequency of the reflected echoes is about 5 THz due to high microwave velocity (1.1×10^8 m/s) and the short device length (10 μm). Since this round-trip frequency is far beyond our measured device bandwidth, as discussed later, the boundary reflection effect does not seriously affect the bandwidth of our device. The current–voltage (I–V) test of the fabricated devices showed ohmic like contact behavior and exhibited very low dark currents ($\sim$1 nA) even under high bias voltage (15 V), implying excellent isolation between electrodes with self-aligned processes.

We employed a mode-locked Ti : sapphire laser as the light source for I–V and EO sampling measurements. The FWHM of optical pulses was 100 fs with 100-MHz repetition rate. For dc photocurrent measurement, the wavelength was tuned to 780 nm. The measured average photocurrent was found to be linearly increased with bias voltage. We applied 15-V maximum bias voltage to avoid device breakdown and damage of microwave bias tee. The measured average photocurrent (solid squares) versus average optical input power at a fixed bias of 15 V is shown in Fig. 2, which has a linear relationship. From the slope of a fitting line (dotted line), we obtained net quantum efficiency of about 8.1% (including coupling loss). This value approaches the theoretical value (without optical coupling loss) of internal quantum efficiency (10%) assuming a 400-nm carrier drift distance, 1×10^5 m/s effective carrier velocity, and 400-fs carrier trapping time [14], [15]. This value is also similar to that of the reported quantum efficiency of LTG-GaAs-based p-i-n TWPD [9].

We used EO sampling technique to perform transient current measurement [16]. Fig. 3(a) shows the measured EO traces at

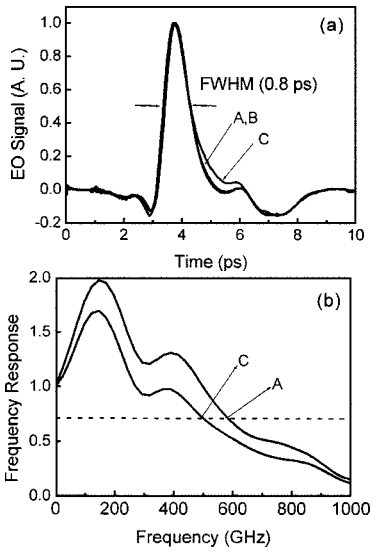

Fig. 3. (a) Measured transient responses with EO sampling technique at a fix bias of 5 V with different average optical input power of 1 mW (trace A), 1.8 mW (trace B), and 2.2 mW (trace C). These traces show 0.8-ps FWHM. (b) Corresponding Fourier transform of the 1- and 2.2-mW traces, which has 570- and 500-GHz 3-dB electrical bandwidth, respectively.

a fixed 5-V bias with different optical input powers. When the average optical input power was below 2.2 mW, there was no significant response broadening and the FWHM of impulse response was about 0.8 ps. At even higher bias, this device can endure more intense optical illumination and deliver even higher output saturation current without bandwidth degradation. Compared with LTG-GaAs p-i-n-based TWPD, whose waveguide width must be kept narrow enough (1 μm) for high-speed performance, MSM-TWPD has higher output saturation current due to its larger photoabsorption volume. By utilizing the impulse response traces in Fig. 3(a) (A and C), we obtained their corresponding Fourier transform traces as shown in Fig. 3(b), which had electrical 3-dB bandwidth of 570 and 500 GHz, respectively. The resonance in frequency domain (200 and 400 GHz) of transformed trace is originated from the negative tail in the time domain trace. In order to minimize the microwave propagation effect (dispersion) on the integrated CPW line during the EO sampling measurement, we performed our measurements as close as possible to the photoabsorption region (the nearest distance was limited by pump–probe interference). One possible origin of the negative tail is the substrate high-order radiation mode from the CPW line structure [17] in the photoabsorption region. The time interval between the peaks of signal and negative tail is 3.6 ps, in agreement with the round-trip time of oblique incidence echo signal [17] due to substrate radiation mode with a substrate thickness of 100 μm. In ordinary LTG-GaAs-based vertically illuminated MSM photodetectors, we usually cannot observe this effect due to longer round-trip time for a 500-μm-thick substrate [17]. With respect to LTG-GaAs-based p-i-n TWPD, this effect does not happen possibly due to electric field confinement in the intrinsic layer with a slow wave mode that made substrate radiation much harder. With optical misalignment, significant decrease in quantum efficiency was observed, however, without any obvious bandwidth degradation [18].

In summary, an ultrahigh-speed MSM-TWPD is proposed and demonstrated, utilizing self-aligned process with LTG-GaAs active region. An impulse response FWHM of 0.8-ps and 570-GHz transformed electrical bandwidth was obtained, with 8.1% net quantum efficiency under 15-V bias. Compared with LTG-GaAs-based p-i-n TWPD, this novel device has similar quantum efficiency and higher output saturation current without significant bandwidth degradation. With a simple fabrication process (without e-beam lithography or complex isolation process) and high-speed high-power performance, this novel device has great potential in the application of terahertz radiation or can be integrated as a distributed PD array for higher electrical output current.

REFERENCES

[1] K. Kato, "Ultrawide-band/high-frequency photodetectors," *IEEE Trans. Microwave Theory Tech.*, vol. 47, pp. 1265–1281, July 1999.

[2] C. L. Goldsmith, G. A. Magel, B. M. Kanack, and R. J. Baca, "Coherent combing of RF signals in a traveling-wave photodetector array," *IEEE Photon. Technol. Lett.*, vol. 9, pp. 998–990, July 1997.

[3] S. Y. Chou and M. Y. Liu, "Nanoscale tera-hertz metal–semiconductor–metal photodetectors," *IEEE J. Quantum Electron.*, vol. 28, pp. 2358–2368, Oct. 1992.

[4] S. J. Wook, C. Caneau, R. Bhat, and I. Adesida, "Application of indium–tin–oxide with improved transmittance at 1 μm for MSM photodetectors," *IEEE Photon. Technol. Lett.*, vol. 5, pp. 1313–1315, 1993.

[5] F. W. Smith, H. Q. Le, V. Diadiuk, M. A. Hollis, A. R. Calawa, S. Gupta, M. Frankel, D. R. Dykaar, G. A. Mourou, and T. Y. Hsiang, "Picosecond GaAs-based photoconductive optoelectronic detectors," *Appl. Phys. Lett.*, vol. 54, pp. 890–892, 1989.

[6] J. F. Holzman, F. E. Vermeulen, and A. Y. Elezzabi, "Ultrafast photoconductive self-switching of subpicosecond electrical pulses," *IEEE J. Quantum Electron.*, vol. 36, pp. 130–136, Feb. 2000.

[7] H. F. Taylor, O. Eknoyan, C. S. Park, K. N. Choi, and K. Chang, "Traveling wave photodetectors," in *Proc. SPIE Optoelectronic Signal Processing for Phased- Array Antennas II*, vol. 1217, 1990, pp. 59–63.

[8] K. S. Giboney, M. J. W. Rodwell, and J. E. Bowers, "Traveling-wave photodetector theory," *IEEE Trans. Microwave Theory Tech.*, vol. 45, pp. 1310–1319, Aug. 1997.

[9] Y. J. Chiu, S. B. Fleischer, and J. E. Bowers, "High-speed low-temperature-grown GaAs p-i-n traveling-wave photodetector," *IEEE Photon. Technol. Lett.*, vol. 10, pp. 1012–1014, 1998.

[10] V. M. Hietala, G. A. Vawter, T. M. Brenan, and B. E. Hammons, "Traveling-wave photodetectors for high-power, large bandwidth applications," *IEEE Trans. Microwave Theory Tech.*, vol. 43, pp. 2291–2297, Sept. 1995.

[11] J. W. Shi and C.-K. Sun, "Design and analysis of long-absorption length traveling-wave photodetector," *J. Lightwave Technol.*, vol. 18, pp. 2176–2187, Dec. 2000.

[12] H. Hasegawa, M. Furukawa, and H. Yanai, "Properties of microstrip line on Si–SiO_2 system," *IEEE Trans. Microwave Theory Tech.*, vol. 19, pp. 869–881, 1971.

[13] K. C. Gupta, R. Garg, I. Bahl, and P. Bhartia, *Microstrip Lines and Slotlines*. Boston: Artech House, 1996.

[14] S. Gupta, J. F. Whitaker, and G. A. Mourou, "Ultrafast carrier dynamics in III–V semiconductors grown by molecular-beam epitaxy at very low substrate temperatures," *IEEE J. Quantum Electron.*, vol. 28, pp. 2464–2472, Oct. 1992.

[15] S. M. Sze, *Physics of Semiconductor Devices*. New York: Wiley, 1985, p. 746.

[16] K. J. Weingarten, M. J. W. Rodwell, and D. M. Bloom, "Picosecond optical sampling of GaAs integrated circuits," *IEEE J. Quantum Electron.*, vol. 24, pp. 198–220, Feb. 1988.

[17] M. Y. Frankel, S. Gupta, J. A. Valdmanis, and G. A. Mourou, "Terahertz attenuation and dispersion characteristics of coplanar transmission lines," *IEEE Trans. Microwave Theory Tech.*, vol. 39, pp. 910–916, June 1991.

[18] C. C. Wang, M. Curie, R. Sobolewski, and T. Y. Hsiang, "Subpicosecond electrical pulse generation by edge illumination of silicon and indium phosphide photoconductive switches," *Appl. Phys. Lett.*, vol. 67, pp. 79–81, 1995.